The Planetary Science Journal, 4:188 (6pp), 2023 October https://doi.org/10.3847/PSJ/acf9f8

The Origin of Jupiter's Obliquity

Rola Dbouk and Jack Wisdom
Department of Earth, Atmospheric and Planetary Sciences, Massachusetts Institute of Technology, Cambridge, MA 02139, USA; rdbouk@mit.edu
Received 2023 July 19; revised 2023 September 11; accepted 2023 September 13; published 2023 October 5

Abstract

The origin of the $3\overset{\circ}{.}12$ obliquity of Jupiter's spin axis to its orbit normal is unknown. Improved estimates of Jupiter's moment of inertia rule out a previously proposed explanation involving a resonance with the precession of the inclined orbit of Uranus. We find that a nonadiabatic crossing of the resonance between Jupiter's spin precession and the $-f_5+f_6+g_6$ mode could have tilted Jupiter to its present-day obliquity starting from a 0° primordial obliquity. This places constraints on the migration rates of the satellites Ganymede and Callisto.

Unified Astronomy Thesaurus concepts: Jupiter (873); Spin-orbit resonances (2296)

1. Introduction

"If the planets grew smoothly and continuously by accreting small bodies and gas from an isolated flat disk, then their obliquities should be zero" (Tremaine 1991). The $3\overset{\circ}{.}12$ obliquity of Jupiter, despite being small, requires an explanation.

The unexpectedly rapid migration of Titan (Lainey et al. 2009) led to new scenarios for the formation of the large $26\overset{\circ}{.}7$ obliquity of Saturn (Saillenfest et al. 2021a; Wisdom et al. 2022), which involve a secular spin–orbit resonance with the precession of Neptune's inclined orbit. Indeed, the rapid migration of Titan rules out all explanations of the large obliquity of Saturn that involve processes in the early solar system. In the scenario of Saillenfest et al. (2021a), the Saturn system is still in the Neptune resonance; and in the scenario of Wisdom et al. (2022), the system is close to but not in the resonance. The latter conclusion was based on new determinations of the moment of inertia of Saturn, based on interior models constrained by Cassini gravity determinations. The moments of inertia found in Wisdom et al. (2022) used very different methods, but were found to be in remarkable agreement with one another. They are supported by more recent independent determinations (Mankovich et al. 2023). The determination by Jacobson (2022) has larger estimated uncertainties, but is also compatible. As pointed out by Ward & Hamilton (2004), if the system is in the secular spin–orbit resonance, then the libration amplitude is nonzero, of order 31°. This in turn implies that the primordial obliquity of Saturn is nonzero, of order 4°. For the primordial obliquity to have been zero, one must appeal to additional phenomena, such as later impacts, to excite the libration amplitude. In the scenario of Saillenfest et al. (2021a), the nonzero libration amplitude also implies that the primordial obliquity of Saturn was nonzero. On the other hand, the scenario of Wisdom et al. (2022) is compatible with zero primordial obliquity.

What then is the origin of Jupiter's obliquity? It is natural to look for an analogous explanation of Jupiter's obliquity involving secular spin–orbit resonances with zero primordial obliquity. Nesvorný (2018) rules out past resonances with Neptune in the early solar system. Ward & Canup (2006) proposed that a near resonance between the precession of Jupiter's spin axis and the nodal precession of the inclined orbit of Uranus could partially explain the obliquity of Jupiter. For this to be the case, they deduced that Jupiter's normalized moment of inertia, $\lambda = C/(MR^2)$, was close to 0.236, where C is the polar moment of inertia, M is the mass, and R is the fiducial equatorial radius of 71,492 km. Based on measured gravitational moments of Jupiter as determined by Juno, Militzer & Hubbard (2023) have determined that the normalized moment of inertia is 0.26393 ± 0.00001. Using the consistent level curve (CLC) method of Wisdom (1996) to fit the Juno gravitational moments, we find a normalized moment of inertia of 0.263932, in remarkable agreement with Militzer & Hubbard (2023; see Appendix A). These values are much larger than the value proposed by Ward & Canup (2006), so their proposed explanation of the obliquity of Jupiter is ruled out. Here we explore the possibility that a different secular spin–orbit resonance excited all or part of Jupiter's obliquity.

2. Other Possible Resonances

Secular spin–orbit resonances occur when the frequency of the precession of the spin axis matches the frequency of a term in the precession of the orbit. As the obliquity of Jupiter remains unexplained by the Uranus resonance, we were led to consider alternate resonances that could explain Jupiter's nonzero obliquity.

For a planet with satellites in a fixed circular orbit, the frequency of precession of the spin axis is $\alpha\cos(\epsilon)$, where ϵ is the obliquity of the spin axis to the orbit normal and α is the precession constant

$$\alpha = \frac{3}{2}\frac{n_J^2}{\omega}\frac{J_2+q}{\lambda+l}, \tag{1}$$

where n_J is the mean motion of Jupiter, ω is the angular frequency of Jupiter's rotation, J_2 is the second gravitational moment of Jupiter, and q and l approximate the contributions of the Galilean satellites to J_2 and λ, respectively, according to

$$q = \frac{1}{2}\sum_j \frac{m_j}{M}\frac{a_j^2}{R^2}\frac{\sin(2(\epsilon - i_j^L))}{\sin(2\epsilon)}$$
$$l = \sum_j \frac{m_j}{M}\frac{a_j^2}{R^2}\frac{n_j}{\omega}\frac{\sin(\epsilon - i_j^L)}{\sin(\epsilon)}, \tag{2}$$

where the subscript j refers to the jth satellite, m_j is its mass, a_j is its semimajor axis, and n_j is its mean motion (Ward 1975;

Table 1
Largest Terms in the Inclination/Precession Motion of Jupiter

Identity	T (yr)	γ (rad day^{-1})	$\log_{10}(\beta)$	δ (rad)
g_8	1872103	-9.18882×10^{-9}	−3.24	0.4105
$f_5 - f_7 + g_7$	703168.7	-2.44641×10^{-8}	−4.96	0.7307
$-f_5 + f_6 + g_6$	553194.4	-3.10965×10^{-8}	−4.76	0.7751
g_7	432749.7	-3.97514×10^{-8}	−3.32	2.4470
g_6	49217.01	-3.49522×10^{-7}	−2.50	5.3644
$f_5 - f_6 + g_7$	48027.74	-3.58177×10^{-7}	−4.63	3.8941

French et al. 1993; Saillenfest et al. 2021b). The angle i_j^L is the inclination of the Laplace plane to the planetary equator (Tremaine et al. 2009); the normal to the Laplace plane is the direction about which the normal to the satellite orbit precesses. The magnitude of i_j^L depends on the planetary oblateness and obliquity, and the semimajor axes involved. The corresponding period of the planet's spin axis precession is $P = 2\pi/(\alpha \cos(\epsilon))$. For Jupiter, the precession constant is dominated by the contributions to q from Ganymede and Callisto. Our estimate of the present-day period of the Jovian spin axis precession is $P = 5.306 \times 10^5$ yr.

Applegate et al. (1986) reported a period of 432,749.7 yr for the Uranus mode g_7. The current system is not close enough to the Uranus resonance to explain the obliquity of Jupiter, as proposed in Ward & Canup (2006). The precession frequency of Jupiter is too low. The outward migration of the satellites increases q, which in turn increases α, based on Equations (1) and (2). The Uranus resonance was not encountered in the past, but may be encountered in the future (Saillenfest et al. 2020).

The secular evolution of Jupiter's orbit can be expressed as a sum of terms (Applegate et al. 1986):

$$\sin\frac{I}{2}\sin\Omega = \sum_j \beta_j \sin(\gamma_j t + \delta_j)$$
$$\sin\frac{I}{2}\cos\Omega = \sum_j \beta_j \cos(\gamma_j t + \delta_j), \quad (3)$$

where I is the orbital inclination of Jupiter with respect to the invariable plane, Ω is the longitude of ascending node of its orbit, t is the time, β_j is the amplitude of the term, γ_j is its angular frequency, and δ_j is a phase. The largest terms in the motion of Jupiter are listed in Table 1.

We see that other possible resonances may have been encountered in the past. The most recent term encountered in the past is identified as the mode combination $-f_5 + f_6 + g_6$ with a period of 553,194.4 yr. We denote by β the amplitude of this term (removing the index). The amplitude of the $-f_5 + f_6 + g_6$ term is $\beta = 10^{-4.76} = 1.74 \times 10^{-5}$ radians. The next most recent term in the past is $f_5 - f_7 + g_7$ with a period of 7,031,698.7 yr. The amplitude of this term is $\beta = 10^{-4.96} = 1.10 \times 10^{-5}$ radians. Table 1 includes all terms listed in Applegate et al. (1986) larger than this amplitude. We have confirmed that the addition of the small term $f_5 - f_6 + g_7$ does not affect our conclusions, justifying the cutoff at this term.

There are two possible outcomes of the resonance passage. If the change in α is slow enough, the system would have been captured in the resonance and the obliquity of Jupiter would be large, which is incompatible with the present low-obliquity nonresonant state. However, if α changes quickly enough, the system would not be captured and the resonance would be crossed. The obliquity will change during the crossing.

A measure of the strength of the resonance is given by the obliquity θ_0 that would have been acquired if the resonance was passed adiabatically in the direction for which capture is not allowed. This is

$$\cos(\theta_0) = \frac{2}{(1 + (\tan(2\beta))^{2/3})^{3/2}} - 1, \quad (4)$$

where $\beta \approx I/2$ is the amplitude of the contribution (Ward & Hamilton 2004). We anticipate that for evolution in the direction for which capture is possible, but which is too rapid for capture to occur, the obliquity that is acquired will be of order θ_0. For the $-f_5 + f_6 + g_6$ resonance, this gives θ_0 of 4°.6, which is comparable to Jupiter's obliquity. This expectation is confirmed by our simulations (see Figure 1).

3. Resonance Model

Since we anticipate that the resonance crossing is not adiabatic, we investigate the crossing with an approximate resonance model that captures the dynamics. The time-averaged Hamiltonian describing the spin axis evolution is (Peale 1969; Touma & Wisdom 1993; Wisdom 2006)

$$H = -\frac{1}{2} MR^2 \lambda \omega \alpha (\cos\epsilon)^2 / (1 - e^2)^{3/2}, \quad (5)$$

where e is Jupiter's orbital eccentricity. The inclination and node of Jupiter are given by Equation (3). The Hamiltonian is expressed in canonical coordinates that define the orientation relative to an inertial reference. We use the nonsingular canonical coordinates of Wisdom (2006). The equations of motion are Hamilton's equations. These equations are numerically integrated.

The resonance occurs when Jupiter's spin precession frequency and the frequency of the mode $-f_5 + f_6 + g_6$ are close. We examine the passage through the resonance with zero initial obliquity by varying the precession constant α linearly, with the rate $\dot{\alpha}$. Figure 1 shows the obliquity of Jupiter at the end of a set of simulations as a function of $\dot{\alpha}$. For $\dot{\alpha} < 3 \times 10^{-16}$ rad yr^{-2}, the system is captured by the resonance and the final obliquity is large; for larger $\dot{\alpha}$, capture does not occur and the resulting obliquities are lower. For these calculations, we only included the resonance term in Equation (3), ignoring rapidly oscillating terms. The black horizontal line is θ_0, the obliquity obtained on reverse adiabatic passage, which we suggested should be comparable to the excitation for nonadiabatic forward passage. The purple curve is the predicted nonadiabatic obliquity in the limit of large $\dot{\alpha}$, which is (Ward et al. 1976; Ward & Hamilton 2004)

$$\theta \to |\gamma|(2\beta)\sqrt{2\pi/\dot{\alpha}}. \quad (6)$$

Notice that the actual nonadiabatic obliquity is larger than Equation (6) and that Equation (6) is invalid if $\dot{\alpha}$ is small enough that capture occurs. For larger $\dot{\alpha}$ (not shown), Equation (6) becomes more accurate. We investigated the resonance passage with β larger and smaller by a factor of 10. In each case, we found that θ_0 was a good estimate of the obliquity obtained for nonadiabatic crossing of the resonance; the largest obliquity obtained for nonadiabatic crossing of the resonance was approximately $2\theta_0$. Further, we found that Equation (6) again underestimated the obliquity near the transition point, but was accurate for large $\dot{\alpha}$. The red

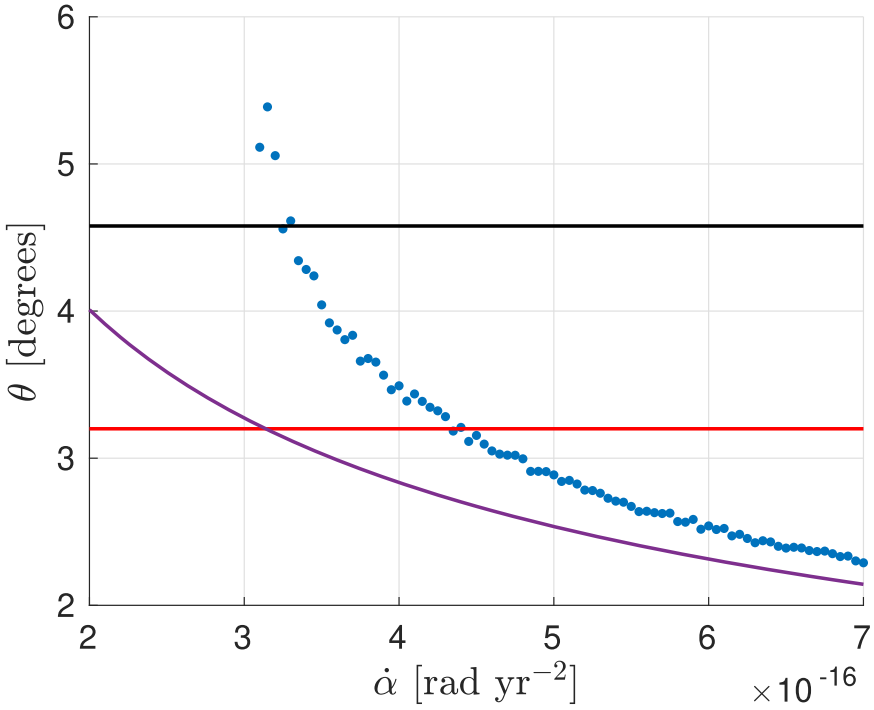

Figure 1. The obliquity, θ, obtained for different $\dot{\alpha}$, the rate of change of the precession constant (blue dots). The black horizontal line is the value of θ_0. The purple curve is Equation (6). The red horizontal line is the mean obliquity of Jupiter.

horizontal line is the 3°.2 mean obliquity of Jupiter at present (see Appendix B). We see that the obliquity of Jupiter can be explained by this nonadiabatic passage. This allows us to estimate $\dot{\alpha}$ at the time of resonance passage. We find $\dot{\alpha} \approx 4.4 \times 10^{-16}$ rad yr^{-2}. The uncertainty is of order 0.1×10^{-16} rad yr^{-2}. If we were to presume this was constant, in order to get an order of magnitude estimate of the time of resonance passage, we find that Jupiter's obliquity was excited roughly 1.4 billion years ago.

4. Constraints on Satellite Evolution

We have determined the rate of change of the precession constant that is required to explain the obliquity of Jupiter. The precession constant increases with time as the satellites migrate outward due to the q and l terms (Equation (2)). The migration rates must be fast enough to avoid capture in the resonance, but slow enough that Jupiter's obliquity is obtained, so this places a constraint on the migration rates of the satellites.

The past migration of the satellites is uncertain. A rapid migration of the Saturnian satellites has been reported (Lainey et al. 2020). This rapid migration is consistent with the resonance-locking hypothesis (Fuller et al. 2016). The migration rates of Io, Europa, and Ganymede have been reported by Lainey et al. (2009). These rates have also been interpreted in terms of the resonance-locking hypothesis in several studies (Downey et al. 2020; Lari et al. 2023). An alternate explanation of the rapid migration of the Jovian and Saturnian satellites has been given by Terquem (2023).

For definiteness, we adopt the resonance-locking expressions for satellite evolution,

$$n(t) = \omega + (n(t_{\rm now}) - \omega)\exp\left(\frac{t - t_{\rm now}}{t_\alpha}\right), \tag{7}$$

where $t_{\rm now}$ is 4.5 Gyr and t_α is the mode evolution timescale (Fuller et al. 2016; Nimmo et al. 2018; Downey et al. 2020).

Approximate q values for Io, Europa, Ganymede, and Callisto are 0.00082, 0.00112, 0.00864, and 0.01640, respectively. The two largest contributions to q are from Ganymede and Callisto because of their large masses and distances to Jupiter. So we will restrict attention to them. A rapid migration rate of Ganymede has been measured (Lainey et al. 2009). The tidal evolution timescale $t_{\rm tide} = a/\dot{a}$. For Ganymede, the observed $t^G_{\rm tide}$ is 9.6 ± 1.6 Gyr (Lainey et al. 2009). Fuller et al. (2016) suggest $t^G_{\rm tide} = 20$ Gyr at present. Callisto's migration has not yet been observed. Downey et al. (2020) and Lari et al. (2023) studied possible histories of the Galilean satellite resonances assuming a fast migration of Callisto, so we will similarly include Callisto's migration and give constraints on its rate. We also consider a case where Callisto is not evolving ($t^C_{\rm tide} = \infty$).

From $t_{\rm tide}$ at present, we compute the mode evolution timescale t_α and hold it fixed. The two timescales are related by (Downey et al. 2020)

$$\frac{1}{t_{\rm tide}} = \frac{2}{3}\frac{1}{t_\alpha}\left(\frac{\omega}{n} - 1\right). \tag{8}$$

For a given $t^G_{\rm tide}$, we compute t^G_α. Note that t_α could be somewhat different for each satellite because each satellite could be resonantly locked to different interior structures (Downey et al. 2020). We use the resonance model (Section 3) to determine t^C_α, the mode timescale for Callisto, so that the resonance is crossed (at time t_c) with the rate required to explain the obliquity of Jupiter. The present tidal evolution timescale for Callisto, $t^C_{\rm tide}$, is then determined. For the case where $t^C_{\rm tide} = \infty$, we determine the required t^G_α and consequently $t^G_{\rm tide}$. The current values of the migration rate $\dot{a}$ for

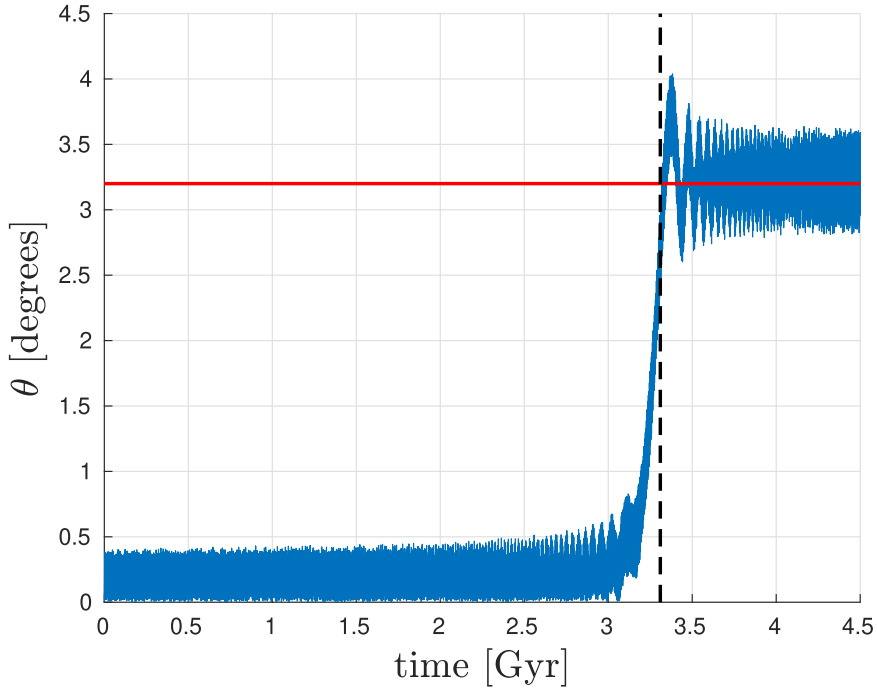

Figure 2. Sample evolution of nonadiabatic resonance crossing leaving Jupiter's obliquity oscillating around the average value (red horizontal line). The vertical dashed line shows the time at which α is equal to the frequency of the $-f_5 + f_6 + g_6$ mode. The parameters of this evolution are from the second line of Table 2.

Table 2
The Migration Parameters for Ganymede and Callisto Required for the Resonance Crossing in the Four Cases Studied

$t^G_{\rm tide}$ (Gyr)	$t^C_{\rm tide}$ (Gyr)	$\dot{a}_G$ (cm yr^{-1})	$\dot{a}_C$ (cm yr^{-1})
38.4	∞	12.8	0
9.6	128.9	11.2	1.5
20.0	25.0	5.4	7.6
∞	12.0	0	15.7

Note. In each case, the crossing time t_c is around 3.3 Gyr.

Ganymede and Callisto are computed from $t_{\rm tide}$ (Table 2). For $t^G_{\rm tide}$ near 20 Gyr, t^G_α and t^C_α are similar.

Downey et al. (2020) suggest a tidal timescale for Callisto of 2.7 Gyr, which is lower than the values we found that explain the obliquity of Jupiter. Such a high rate of migration would not have allowed Jupiter's obliquity to develop by this mechanism. By artificially choosing $t^G_{\rm tide} = \infty$, we deduce an upper limit on the migration rate of Callisto of 15.7 cm yr^{-1}. This corresponds to a lower limit on the Q of Jupiter at Callisto's frequency of about 8 (for $k_2 = 0.379$), which is potentially measurable by future missions, such as the JUICE mission (Dirkx et al. 2017). If Callisto is not involved in a resonance lock, then $\dot{a}_C$ would be small. Terquem (2023) also predicts a small $\dot{a}_C$ of order 0.01 cm yr^{-1}. The case where Callisto is not migrating provides an upper limit on the migration rate of Ganymede, which we deduce to be 12.8 cm yr^{-1}.

Alternatively, we can consider a simplified model in which $\dot{\alpha}$ is constant and assume it is entirely due to the evolution of Ganymede. In this case, we find an upper limit of 10.2 cm yr^{-1}. The measured value by Lainey et al. (2009) is 11.2 ± 1.9 cm yr^{-1}, which is compatible with our determinations of the upper limit. If there was a small primordial obliquity of Jupiter, then our upper limits could be somewhat relaxed.

Figure 2 shows a sample evolution where the final obliquity of Jupiter oscillates around the present mean value, shown as the horizontal line red line. For this calculation, we included all the terms in Table 1 and the resonance-locking expressions for the evolution of the satellites. For these parameters, the system is captured in the Uranus resonance about 2.5 Gyr in the future and the obliquity of Jupiter then rises dramatically.

The late time of resonance crossing, only around 1.2 billion years ago, is consistent with the fact that we have ignored the initial phase in which the solar system frequencies are changing and the change of the precession constant due to the early contraction phase of Jupiter (Ward & Hamilton 2004).

5. Conclusion

The obliquity of Jupiter could have been established by a nonadiabatic crossing of the resonance between Jupiter's spin precession and the mode $-f_5 + f_6 + g_6$. The rate of change of the precession constant, $\dot{\alpha}$, must be $\approx 4.4 \times 10^{-16}$ rad yr^{-2} at the time of crossing to explain the present-day obliquity. With rapidly migrating satellites, such an $\dot{\alpha}$ occurs well after any early phase of planetary instability. We find upper limits on the migration rates of Ganymede and Callisto that explain the obliquity of Jupiter by this mechanism. If we use the resonance-locking model to determine the migration rates of the satellites, we find an upper limit on Ganymede's migration of 12.8 cm yr^{-1} and an upper limit on Callisto's migration of 15.7 cm yr^{-1}. Assuming a constant $\dot{\alpha}$ model, we find an upper limit on Ganymede's migration of 10.2 cm yr^{-1}.

Acknowledgments

Thanks to Francis Nimmo and Caroline Terquem for helpful discussions. This research was supported by NASA's SSW program.

Appendix A
Moment of Inertia of Jupiter

A discussion of prior estimates of the moment of inertia of Jupiter is given by Militzer & Hubbard (2023).

Wisdom (1996) developed the CLC method and used it to find an interior model of Jupiter that fit the gravitational moments as determined by Voyager. The reported normalized moment of inertia for Jupiter was 0.2640. But this value was rounded for the table; the actual value that was found in 1996 was 0.26397.

We have updated the model to fit the gravitational moments of Jupiter determined by Juno (Durante et al. 2020; Militzer & Hubbard 2023; see Table A1). The rotation parameter is $q_{\rm rot} = 0.08919543238$. The input value of the q_0 parameter (called q in Wisdom 1996) for the CLC method is $q_0 = 0.083246414497210167$. The fit value of $q_{\rm rot}$ is 0.08919623036. We used 15-point Chebychev interpolation for the radial functions and extended the solution to degree 6. The fit values of the coefficients in the equation of state are: $\zeta_1 = 1.8556180032843457$, $\zeta_2 = 0.10341538866205373$, and $\zeta_3 = 0.07346385930289676$. The small discrepancy in J_6 is likely due to differential rotation (Militzer & Hubbard 2023).

The normalized moment of inertia for the updated CLC model is 0.263932, in remarkable agreement with the value 0.26393 ± 0.00001 determined by Militzer & Hubbard (2023). The CLC method uses an abstract polynomial equation of state, with coefficients chosen to match the observed gravitational moments; the model of Militzer & Hubbard (2023) uses the CMS method and a physics-based equation of state to fit the gravitational moments. Evidently, the gravitational moments provide a tight constraint on the moment of inertia.

Table A1
Jupiter's Gravitational Moments Reported by Durante et al. (2020), with Those Obtained with the CLC Method

	Measured	CLC Values
$J_2 \times 10^6$	14696.5063 ± 0.0006	14696.50633
$J_4 \times 10^6$	-586.6085 ± 0.0008	−586.60367
$J_6 \times 10^6$	34.2007 ± 0.0022	34.5161

Appendix B
Mean Obliquity of Jupiter

The current obliquity of Jupiter to its orbit is 3°.1 (Ward & Canup 2006), but what is more important is the mean obliquity over million year timescales. The mean obliquity of Jupiter depends on its moment of inertia. With the refined estimate of the moment of inertia of Jupiter, we can now compute the mean obliquity to the invariable plane using full numerical integrations. We use the numerical model of Wisdom et al. (2022), with parameters and orbits derived from Folkner & Park (2018). We include the four Galilean satellites, the four outer planets, and the Sun. We integrate Jupiter as a rigid body. Figure B1 shows the evolution of Jupiter's obliquity 65 Myr into the future. The obliquity evolution shown in Figure B1 is complex, warranting the use of full numerical integrations to determine the mean obliquity of Jupiter. Over this interval, the mean obliquity to the invariable plane is 3°.2.

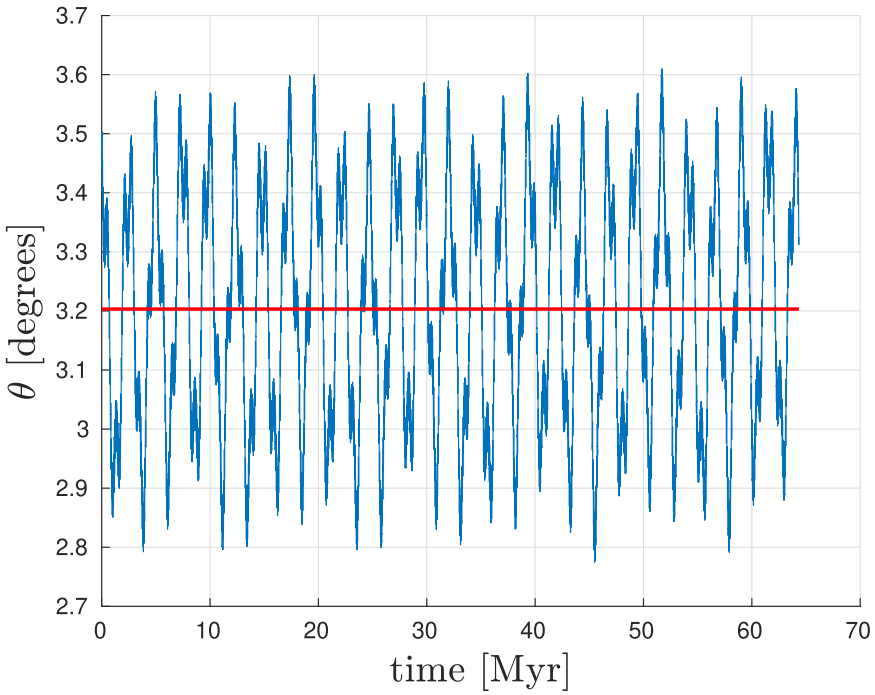

Figure B1. The evolution of θ, the obliquity of Jupiter relative to the invariable plane, obtained by running nbody integrations without satellite migrations. The origin of time is that of J2000 (JD 2451545.0).

ORCID iDs

Rola Dbouk https://orcid.org/0000-0003-4423-1647
Jack Wisdom https://orcid.org/0000-0002-6142-0653

References

Applegate, J. H., Douglas, M. R., Gursel, Y., Sussman, G. J., & Wisdom, J. 1986, AJ, 92, 176
Dirkx, D., Gurvits, L. I., Lainey, V., et al. 2017, P&SS, 147, 14
Downey, B. G., Nimmo, F., & Matsuyama, I. 2020, MNRAS, 499, 40
Durante, D., Parisi, M., Serra, D., et al. 2020, GeoRL, 47, e2019GL086572
Folkner, W., & Park, R. 2018, Planetary and Lunar Ephemeris File DE438, https://naif.jpl.nasa.gov/pub/naif/generic_kernels/spk/planets/de438.bsp
French, R. G., Nicholson, P. D., Cooke, M. L., et al. 1993, Icar, 103, 163
Fuller, J., Luan, J., & Quataert, E. 2016, MNRAS, 458, 3867
Jacobson, R. A. 2022, AJ, 164, 199
Lainey, V., Arlot, J.-E., Karatekin, Ö., & Van Hoolst, T. 2009, Natur, 459, 957
Lainey, V., Casajus, L. G., Fuller, J., et al. 2020, NatAs, 4, 1053
Lari, G., Saillenfest, M., & Grassi, C. 2023, MNRAS, 518, 3023
Mankovich, C. R., Dewberry, J. W., & Fuller, J. 2023, PSJ, 4, 59
Militzer, B., & Hubbard, W. B. 2023, PSJ, 4, 95
Nesvorný, D. 2018, ARA&A, 56, 137
Nimmo, F., Barr, A. C., Behounková, M., & McKinnon, W. B. 2018, in Enceladus and the Icy Moons of Saturn, ed. P. M. Schenk et al. (Tucson, AZ: Univ. Arizona Press), 79
Peale, S. J. 1969, AJ, 74, 483
Saillenfest, M., Lari, G., & Boué, G. 2021a, NatAs, 5, 345
Saillenfest, M., Lari, G., Boué, G., & Courtot, A. 2021b, A&A, 647, A92
Saillenfest, M., Lari, G., & Courtot, A. 2020, A&A, 640, A11
Terquem, C. 2023, MNRAS, 525, 508
Touma, J., & Wisdom, J. 1993, Sci, 259, 1294
Tremaine, S. 1991, Icar, 89, 85
Tremaine, S., Touma, J., & Namouni, F. 2009, AJ, 137, 3706
Ward, W. R. 1975, AJ, 80, 64
Ward, W. R., & Canup, R. M. 2006, ApJL, 640, L91
Ward, W. R., Colombo, G., & Franklin, F. 1976, Icar, 28, 441
Ward, W. R., & Hamilton, D. P. 2004, AJ, 128, 2501
Wisdom, J. 1996, Non-perturbative Hydrostatic Equilibrium, https://hdl.handle.net/1721.1/144248
Wisdom, J. 2006, AJ, 131, 1864
Wisdom, J., Dbouk, R., Militzer, B., et al. 2022, Sci, 377, 1285